PROCEEDINGS OF SCIENCE

Resonance results with the ALICE experiment in pp and Pb-Pb collisions at LHC energies

Sergey Kiselev* **for the ALICE collaboration**
Institute for Theoretical and Experimental Physics, Moscow, Russia
E-mail: Sergey.Kiselev@cern.ch

Short lived resonances have been reconstructed from their hadronic decay with the ALICE experiment at LHC. In pp collisions mesonic $K^*(892)^0$, $\phi(1020)$ and baryonic $\Sigma(1385)$ resonances have been analyzed. For Pb-Pb collisions results on the mesonic resonances are presented. Transverse momentum spectra, yields, particle ratios and comparison with Monte Carlo model predictions are discussed.

XXI International Baldin Seminar on High Energy Physics Problems,
September 10-15, 2012
JINR, Dubna, Russia

*Speaker.

PoS(Baldin ISHEPP XXI)054

1. Introduction

Resonance production plays an important role both in elementary and in heavy-ion collisions. In pp collisions, it provides a reference for tuning event generators inspired by Quantum Chromodynamics (QCD) and the baseline for nuclear collisions. In heavy-ion collisions, the in-medium effects related to the high density and/or high temperature of the medium can modify the properties of short-lived resonances such as their masses, widths, and even their spectral shapes [1]. Moreover, due to short life time the regeneration and rescattering effects become important and can be used to estimate the timescale between chemical and kinetic freeze-out [2].

2. The ALICE detector

The ALICE detector [3] at the LHC is designed to study both Pb-Pb and pp collisions at the TeV-scale centre of mass energy. The components of the ALICE detector most directly related to the results presented here are shortly described below. The Inner Tracking System (ITS) is a silicon detector that surrounds the interaction point and covers the pseudorapidity region $|\eta| < 2$. It is used to reconstruct the collision vertex and provides tracking and particle identification. Particle tracking is mainly provided by Time Projection Chamber (TPC). The TPC also allows particles to be identified through their energy loss. The Time-of-Flight Detector (TOF) sits outside the TPC and measures the time-of-flight of the particles, allowing for additional identification. Both the TPC and the TOF cover the central pseudorapidity region $|\eta| < 0.9$. A pair of scintillation hodoscopes, the VZERO detectors ($2.8 < \eta < 5.1$ and $-3.7 < \eta < -1.7$), were used for event triggering and centrality selection for Pb-Pb collisions.

3. Analysis Procedure

The data analysis was carried out using the collisions recorded by ALICE during 2010, with a sample size ranging for pp collisions at $\sqrt{s} = 7$ TeV from 60 to 210 million events (for the different resonances analyzed) and 10 million events for Pb-Pb collisions at $\sqrt{s_{\rm NN}} = 2.76$ TeV. The resonances have been identified via their main hadronic decay channel: $\mathrm{K}^*(892)^0 \to \pi^\pm + \mathrm{K}^\mp$, $\phi(1020) \to \mathrm{K}^+ + \mathrm{K}^-$, $\Sigma(1385)^\pm \to \Lambda + \pi^\pm$. Due to their very short life time, resonance decay products cannot be distinguished from the particles coming from the primary vertex, and their yield can only be measured by first computing the invariant mass spectrum of all primary candidate's track pairs and then subtracting the combinatorial background. The combinatorial background was evaluated using the event-mixing technique or the like-sign technique. The signal after the combinatorial background subtraction was then fitted with a Breit-Wigner function or a Voigtian function (convolution of Breit-Wigner and Gaussian which accounts for the detector resolution) plus a polynomial for the residual background. After the signal is extracted, the raw yield is evaluated as the integral of the signal function. The raw yields extracted in different $p_{\rm T}$ bins are corrected for efficiency and acceptance and the differential transverse momentum spectra are obtained. The corrected spectra are fitted with a Levy-Tsallis function [4] (pp collisions) or with a Blast Wave function [5], in order to extract the mean transverse momentum $\langle p_{\rm T} \rangle$ and $p_{\rm T}$-integrated yields. The analysis of the $\mathrm{K}^*(892)^0$ and $\phi(1020)$ mesons in pp collisions at $\sqrt{s} = 7$ TeV are described in detail in [6].

4. Results

4.1 pp collisions at $\sqrt{s} = 7$ TeV

The decay products are identified using different combinations of the TPC and TOF information. For the $\phi(1020)$ and $\Sigma(1385)$ the combinatorial background was evaluated using the event-mixing technique, while for the $K^*(892)^0$ the like-sign technique was used. The signal after the background subtraction was then fitted with a Breit-Wigner function for $K^*(892)^0$ and $\Sigma(1385)$ or a Voigtian function for $\phi(1020)$ plus a polynomial for the residual background. Examples of the invariant mass spectra are presented in Fig. 1. Masses and widths of resonances are close to the

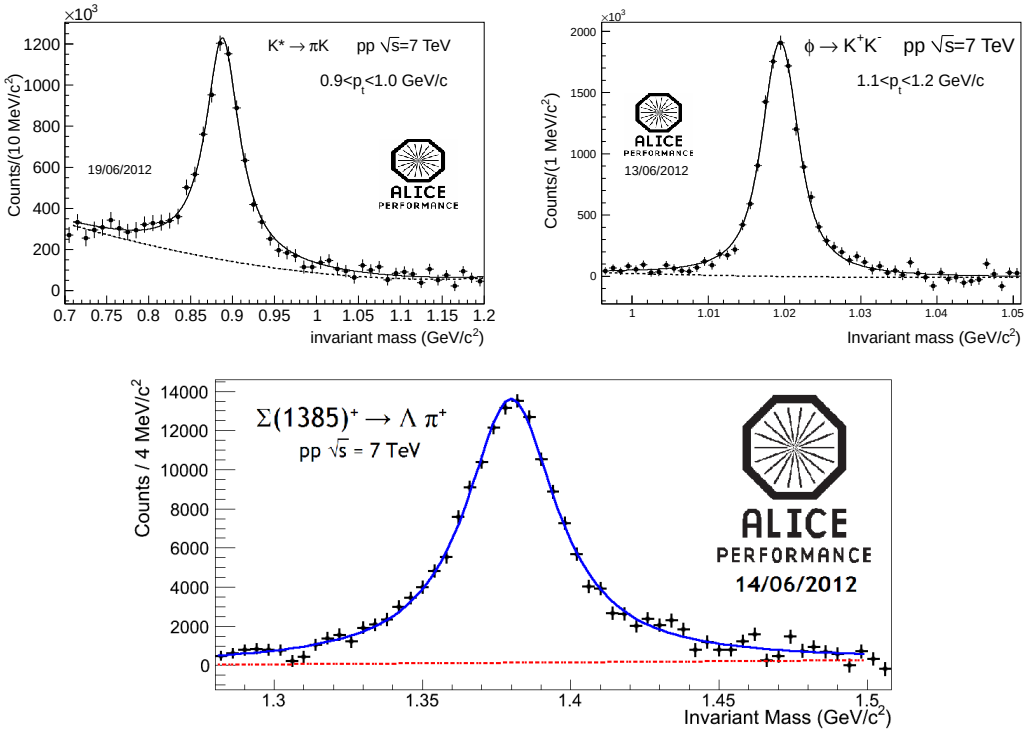

Figure 1: (color online) Signals after the combinatorial background subtraction. The fitting function is the sum of a Breit-Wigner function for $K^*(892)^0$ and $\Sigma(1385)$ or a Voigtian function for $\phi(1020)$ and a polynomial.

PDG values [7], as illustrated in Fig. 2 for the $\Sigma(1385)$

Figure 3 shows the $\phi(1020)$ and $\Sigma(1385)$ spectra with a comparison to a number of PYTHIA [8] tunes and PHOJET [9]. For the $\phi(1020)$ the best agreement is found for the PYTHIA Perugia 2011 tune, which reproduces the high p_T part ($p_T > 3$ GeV/c) rather well. PHOJET and ATLAS-CSC very significantly overestimate the low momentum part ($p_T < 1$ GeV/c) of the transverse momentum distribution but reproduce the high momentum distribution well. The PYTHIA D6T tune gives the best description at low p_T, but deviates from the data at $p_T > 2$ GeV/c. Finally, the PYTHIA Perugia 0 tune underestimates the meson yield for p_T larger than 0.5 GeV/c. The $\Sigma(1385)$ spectrum is well described by the PYTHIA ATLAS-CSC tune for $p_T > 2$ GeV/c, while other models underpredict the data. None of the models gives a fully satisfactory description of the data.

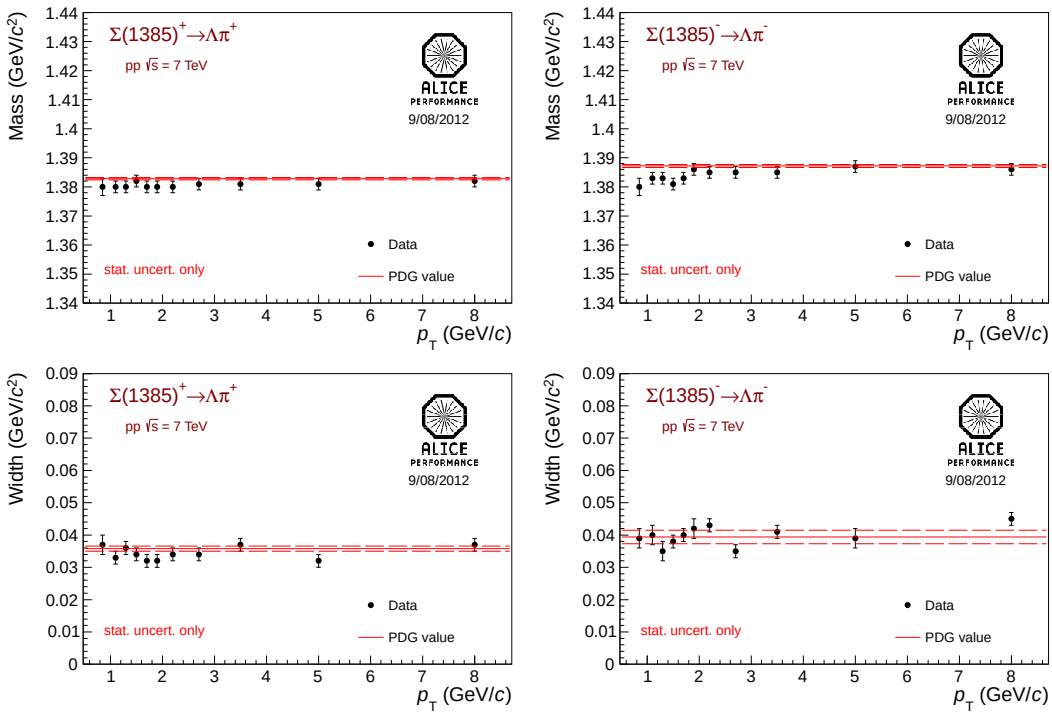

Figure 2: (color online) Mass (top) and width (bottom) of the $\Sigma(1385)^+$ (left) and $\Sigma(1385)^-$ (right) in pp collisions at $\sqrt{s} = 7$ TeV as a function of transverse momentum.

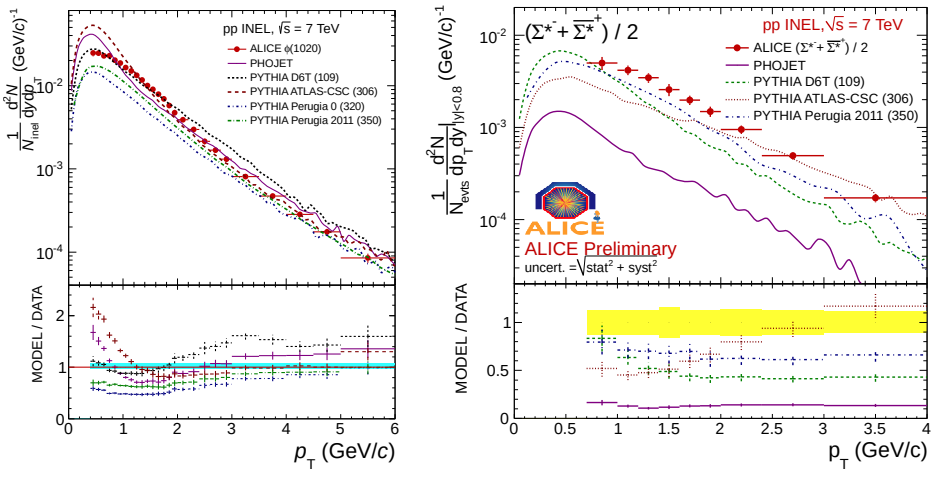

Figure 3: (color online) Comparison of transverse momentum spectra of $\phi(1020)$ [6] and Σ^* in inelastic pp collisions at $\sqrt{s} = 7$ TeV with PHOJET and PYTHIA tunes D6T, ATLAS-CSC, Perugia 0, and Perugia 2011.

The $\langle p_{\mathrm{T}} \rangle$ of $\phi(1020)$ and $\Sigma(1385)$ are presented in Fig. 4, as a function of the particle mass and compared with the value at 900 GeV from ALICE [10] and at 200 GeV from STAR [11, 12]. The $\langle p_{\mathrm{T}} \rangle$ is also in agreement with the trend drawn by other particles at 7 TeV from ALICE [13], which in turn differs from the ISR parametrization (for pions, kaons and protons at $\sqrt{s} = 25$ GeV) [14].

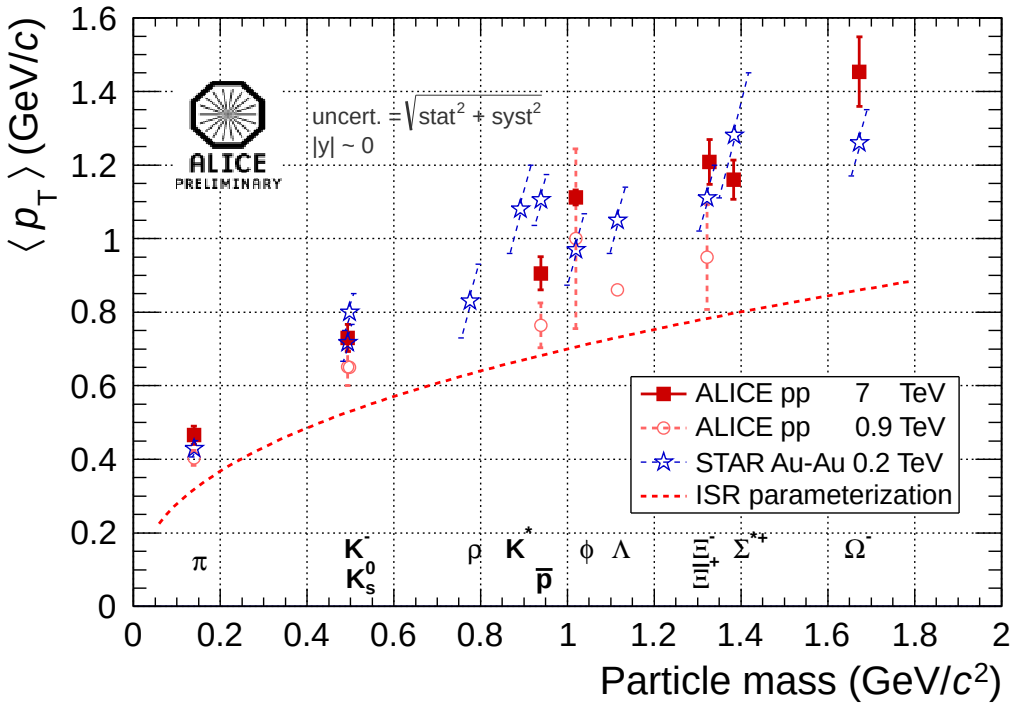

Figure 4: (color online) Mean transverse momentum as a function of the particle mass.

Particle ratios in pp collisions are important as a baseline for comparison with heavy-ion collisions. In heavy-ion collisions, the yields for stable and long-lived hadrons reflect the thermodynamic conditions (temperature, chemical potentials) at chemical freeze-out, whereas the yield for short-lived resonances can be modified by final state interactions inside the hot and dense reaction zone. These ratios are shown in Figs. 5 and 6, together with the results obtained at lower incident energies in pp, e^+e^-, and A-A collisions. The K^*/K^-, ϕ/K^- and ϕ/K^{*1} ratios are essentially independent of energy and also independent of the collision system, with the exception of K^*/K and ϕ/K^* at RHIC [12, 23, 25, 26], where these ratios in nuclear collisions are respectively lower and higher than in pp. On the contrary, the ϕ/π ratio increases with energy both in heavy-ion and in pp collisions up to at least 200 GeV. However, in heavy-ion collisions at $\sqrt{s_{\mathrm{NN}}} = 200$ GeV, the value obtained by the PHENIX experiment [27] is about 40% lower than the STAR result [12], indicating a saturation of this ratio at the RHIC energies. In pp collisions we observe a saturation of the ϕ/π ratio, with no significant change over the LHC energy range between 0.9 and 7 TeV.

In microscopic models where soft particle production is governed by string fragmentation, strange hadron yields are predicted to depend on the string tension [39]. Multi-strange baryons, and

[1] We denote by K^* the average of $K^*(892)^0$ and $\overline{K^*(892)^0}$

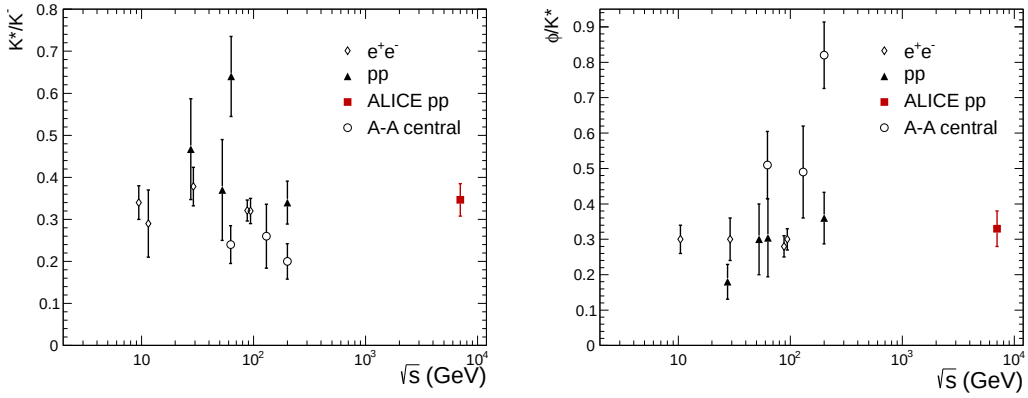

Figure 5: (color online) Energy dependence of particle ratios in e^+e^- (diamonds) [15, 16, 17, 18, 19], and pp (triangles) [11, 12, 20, 21, 22, 23] collisions. Red squares represent the data from the ALICE experiment for 7 TeV pp collisions [6], K^- yields are from [24]. Open circles represent the same ratios in central nucleus-nucleus collisions from [11, 12, 23, 25, 26]. Some points have been displaced horizontally for better visibility.

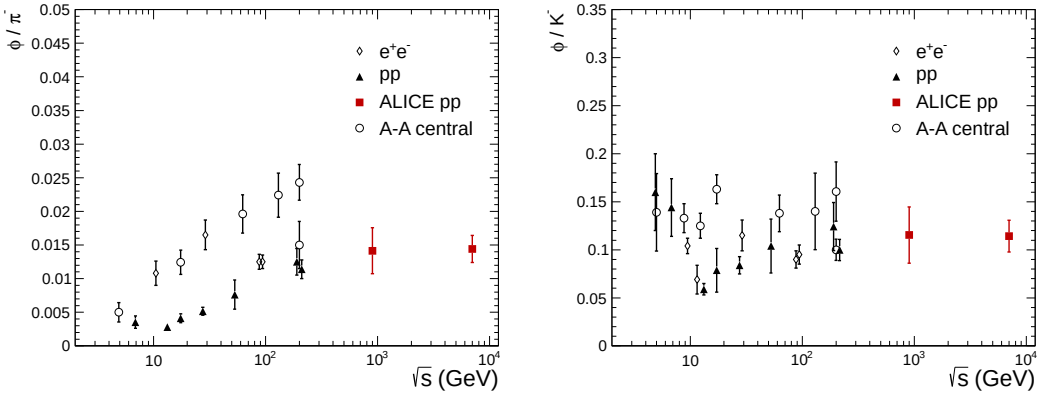

Figure 6: (color online) Energy dependence of the ϕ/π^- and ϕ/K^- ratio in nuclear (open circles) [12, 25, 27, 28, 29, 30, 31], e^+e^- (diamonds) [15, 16, 17, 18, 19], and pp (triangles) [11, 12, 20, 32, 33, 21, 28, 29, 30, 34] collisions. Other π^- and K^- yields are from [35, 34, 36, 37]. Red squares represent the ALICE data at 0.9 and 7 TeV [6]. The π^- and K^- yields at 7 TeV are from [24]. The ϕ, π^-, and K^- yields at 0.9 TeV are from [10, 38]. Some points have been displaced horizontally for better visibility.

in particular the ratio Ω/ϕ , are expected to be very sensitive to the string tension [40]. The ϕ yield is compared to the $\Omega^- + \overline{\Omega}^+$ data measured by ALICE at the same incident energy [13] in Fig. 7 as a function of transverse momentum. The full line represents the PYTHIA model (Perugia 2011 tune), which is a factor 1.5-5 below the data. While this tune describes the ϕ spectrum reasonably well above 2-3 GeV/*c*, it underpredicts multistrange baryon yields by a large factor [13]. The dashed line, which is very close to the data, represents the prediction of a model with increased string tension, the HIJING/B$\overline{\text{B}}$ v2.0 model with a Strong Colour Field (SCF), for pp collisions at 5.5 TeV [40]. This is a model that combines multiple minijet production via perturbative QCD

with soft longitudinal string excitation and hadronization. In this case the SCF effects are modeled by varying the effective string tensions that controls the $q\bar{q}$ and $qq\bar{q}\bar{q}$ pair creation rates and the strangeness suppression factor. The value of string tension used in this calculation is k =2 GeV/fm, equal to the value used to fit the high baryon/meson ratio at $\sqrt{s} = 1.8$ TeV reported by the CDF collaboration [41]. The same calculation at 7 TeV yields a $\sim$ 10% higher ratio [42]. Higher values of the string tension ($\sim$ 3 GeV/fm) also successfully reproduce the $(\Omega^- + \overline{\Omega}^+)/\phi$ ratio in Au-Au collisions at $\sqrt{s} = 200$ GeV [40], but overestimate the $(\Lambda + \overline{\Lambda})/\mathrm{K}^0_S$ at 7 TeV [39].

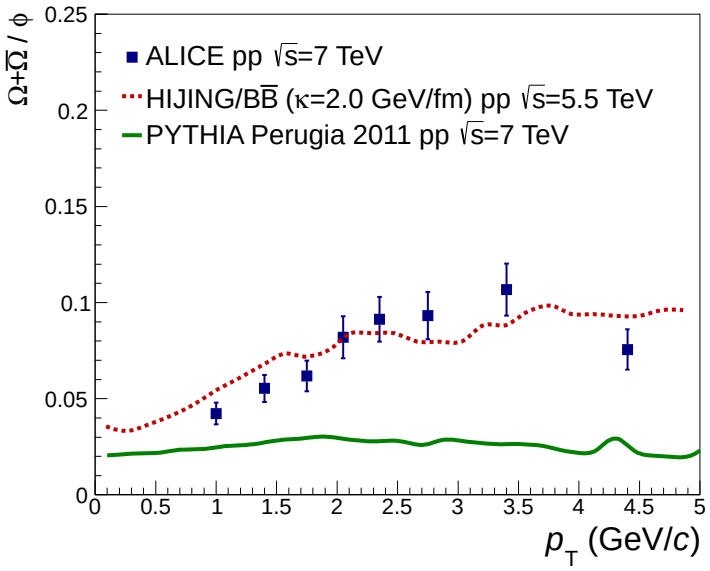

Figure 7: (color online) $(\Omega^- + \overline{\Omega}^+)/\phi$ ratio as a function of transverse momentum for pp collisions at $\sqrt{s} = 7$ TeV [6]. Ω data are from [13]. The dashed line represents the prediction of HIJING/B$\overline{\mathrm{B}}$ v2.0 model with a SCF for pp collisions at $\sqrt{s} = 5.5$ TeV with a string tension of 2 GeV/fm [40]. The same calculation at 7 TeV yields a $\sim$ 10% higher ratio [42]. The full line represents the prediction of the PYTHIA Perugia 2011 tune [43] for pp collisions at $\sqrt{s} = 7$ TeV.

Figure 8 shows the Σ^*/π^-, Σ^*/K^- and Σ^*/Ξ^- ratios as a function of beam energy. The STAR data from [11, 44, 45] have been included. Σ^*/π^- and Σ^*/K^- ratios are independent of energy within errors, the Σ^*/Ξ^- ratio decreases with energy. The data at LHC are compared with thermal model [46] results, assuming a chemical temperature of 170 MeV. The model predictions agree with the measured ratios for Σ^*/π^- and Σ^*/K^- while the prediction for Σ^*/Ξ^- is larger than the measured value.

4.2 Pb-Pb collisions at $\sqrt{s_{\mathrm{NN}}}$ = 2.76 TeV

The decay products are identified using TPC energy loss measurements. For the K^* (ϕ) meson, the combinatorial background is calculated using the like-charge (event mixing) method, the residual background is parametrized using a polynomial, and the peaks are fitted using a Breit-Wigner function. Examples of the invariant mass spectra are presented in Fig. 9.

The masses and widths of the K^* and ϕ mesons, Fig. 10, were extracted from the Breit-Wigner peak fits. The K^* mass is within 10 MeV/c^2 from the PDG value, and a similar difference is

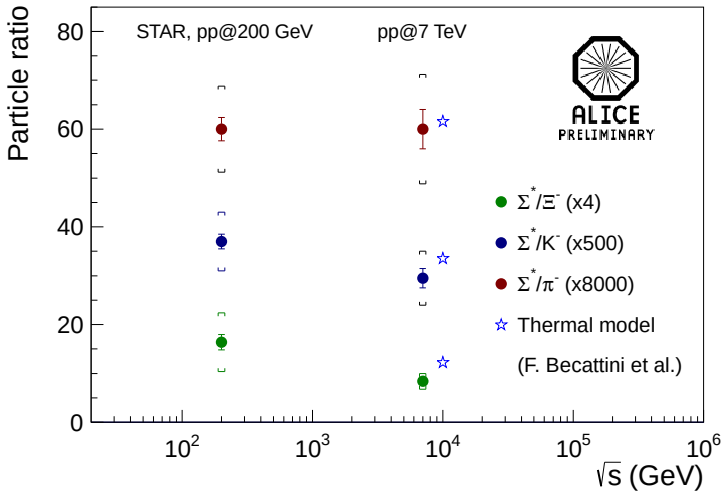

Figure 8: (color online) Σ^*/π^-, Σ^*/K^- and Σ^*/Ξ^- ratios in pp collisions at LHC and RHIC energies with predictions of the thermal model [46].

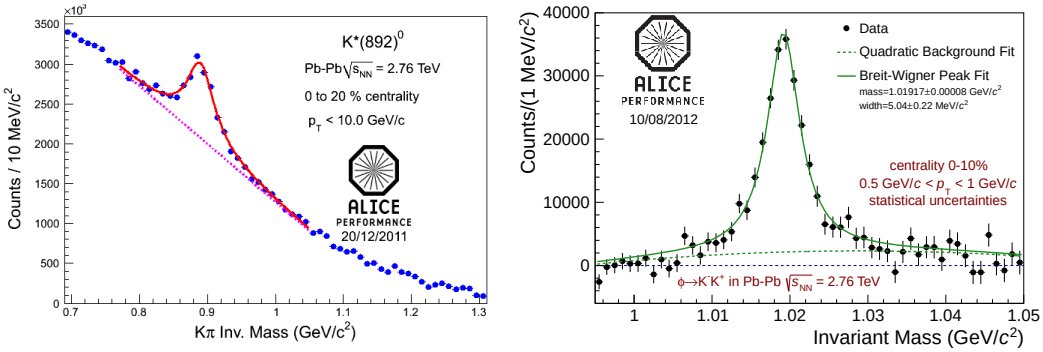

Figure 9: (color online) Signals after the background subtraction for the K^* (left) and ϕ (right) mesons. The fitting function is the sum of a Breit-Wigner function and a polynomial.

observed in pp collisions, indicating an instrumental effect. The K^* width is consistent with the vacuum value. The ϕ mass (width) deviates from the vacuum value by 0.5 (1-2) MeV/c^2. When simulated ϕ peaks are fitted using the same procedure, similar deviations from the vacuum value are observed. There is no apparent centrality dependence in the mass or width.

For every centrality bin spectra have been corrected for the efficiency $\times$ acceptance, the particle identification cuts and the branching ratios. Figure 11 shows corrected transverse momentum spectra for the K^* and ϕ mesons in several centrality bins.

The mean transverse momentum as a function of the mean number of participating nucleons $\langle N_{\mathrm{part}} \rangle$ are shown in Fig. 12. The Pb-Pb results are compared with the measurements in pp collisions at 7 TeV and lower energy measurements at RHIC [23, 47]. The $\langle p_{\mathrm{T}} \rangle$ at LHC energies are higher than that observed at RHIC energies.

Figure 13 shows the particle yield ratios $\mathrm{K}^*/\mathrm{K}^-$, ϕ/π and ϕ/K as a function of $\langle N_{\mathrm{part}} \rangle$ in

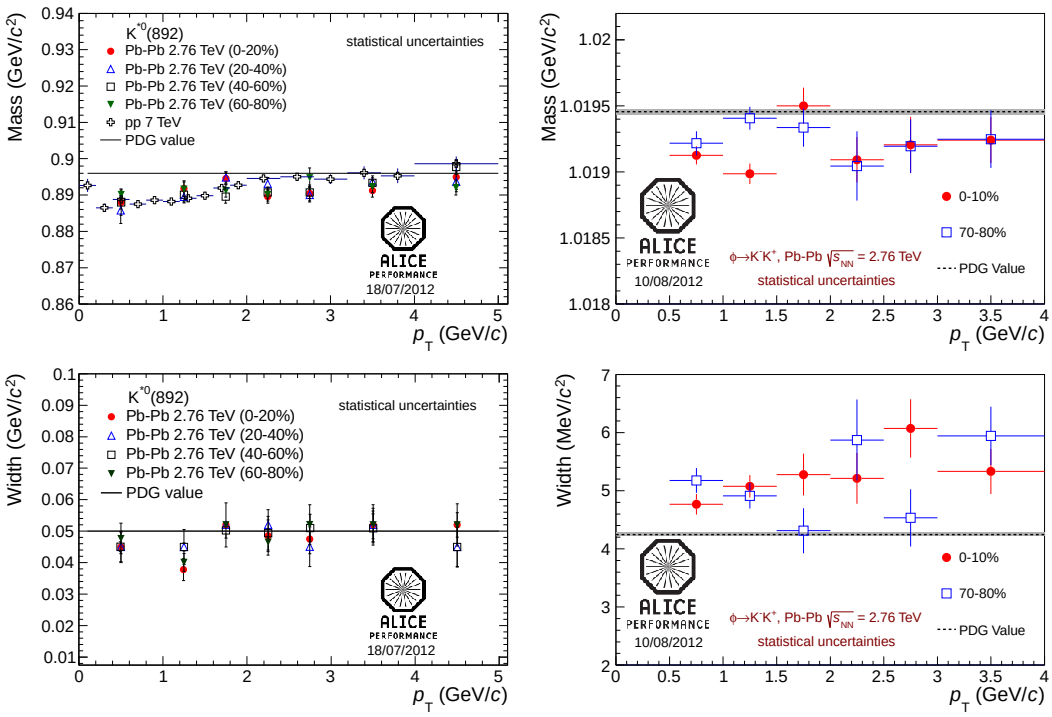

Figure 10: (color online) Mass (top) and width (bottom) of the K* (left) and ϕ (right) in Pb-Pb collisions at $\sqrt{s_{\rm NN}}$ = 2.76 TeV as a function of transverse momentum.

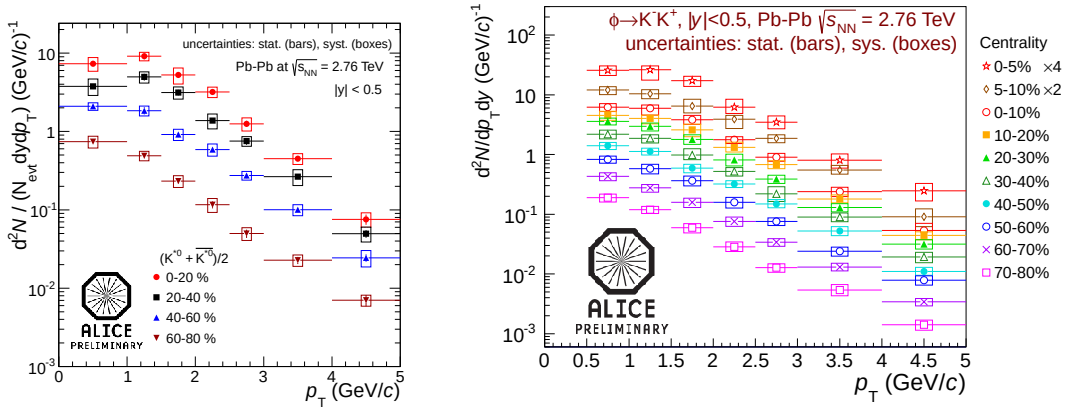

Figure 11: (color online) Transverse momentum spectra of the K* (left) and ϕ (right) mesons in Pb-Pb collisions at $\sqrt{s_{\rm NN}}$ = 2.76 TeV in several centrality bins.

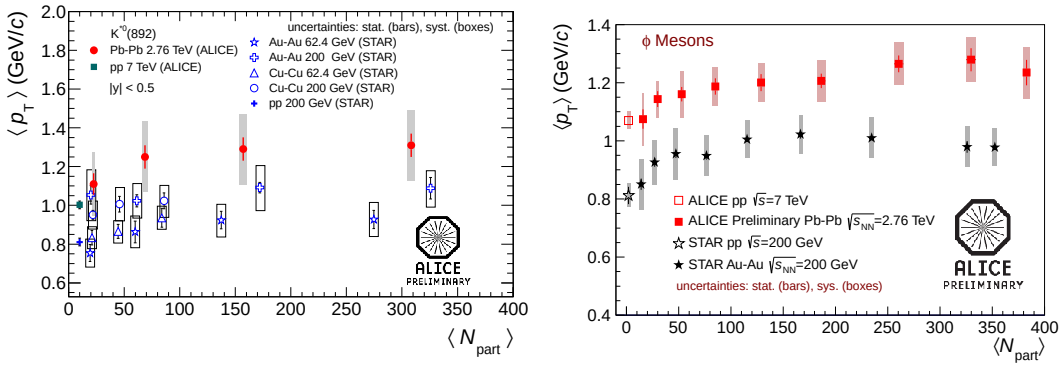

Figure 12: (color online) Mean transverse momentum of the K^* (left) and ϕ (right) mesons as a function of the mean number of participating nucleons $\langle N_{\rm part}\rangle$ in Pb-Pb collisions at $\sqrt{s_{\rm NN}}$ = 2.76 TeV. The results are compared with the pp measurements at $\sqrt{s}$ = 7 TeV and also with the lower energy measurements($\sqrt{s}$ = 200 GeV) at RHIC.

Pb-Pb collisions at $\sqrt{s_{\rm NN}}$ = 2.76 TeV. A weak centrality dependence is observed in the K^*/K^- ratio, while the ϕ/π and ϕ/K ratios are independent of the collision centrality. The decreasing trend in the K^*/K^- ratio suggests a possible increase of hadronic rescattering in the most central collisions. A naive expectation from a kaon coalescence model [48] is an increase in the ϕ/K ratio with increasing collision centrality, which is not seen in our data.

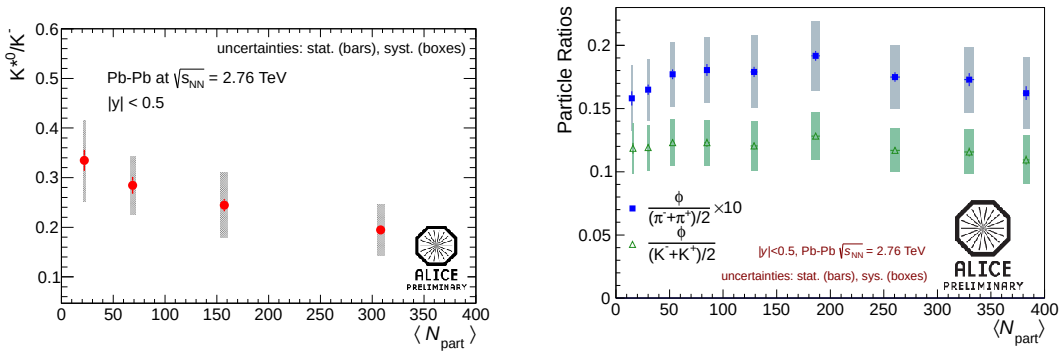

Figure 13: (color online) Particle ratios for the K^* (left) and ϕ (right) mesons as a function of the mean number of participating nucleons $\langle N_{\rm part}\rangle$ in Pb-Pb collisions at $\sqrt{s_{\rm NN}}$ = 2.76 TeV.

The beam energy dependence of particle yield ratios is presented in Fig. 14. The results are compared with lower energy measurements at SPS [29] and RHIC [49] and also with the pp measurements [6]. The particle ratios , ϕ/π and K^*/K^- are found to be independent of beam energy. The K^*/K^- ratio in Pb-Pb collisions is smaller than the one measured in pp collisions. This observation may also indicate the effect of hadronic rescattering at LHC energies. The statistical thermal model of [50] has been used to predict particle yields in central Pb-Pb collisions at $\sqrt{s_{\rm NN}}$ = 2.76 TeV, assuming a temperature of 164 MeV. The model prediction (without rescattering) for ϕ/K is consistent with the measured value, while the prediction for ϕ/π is larger than the measured

value.

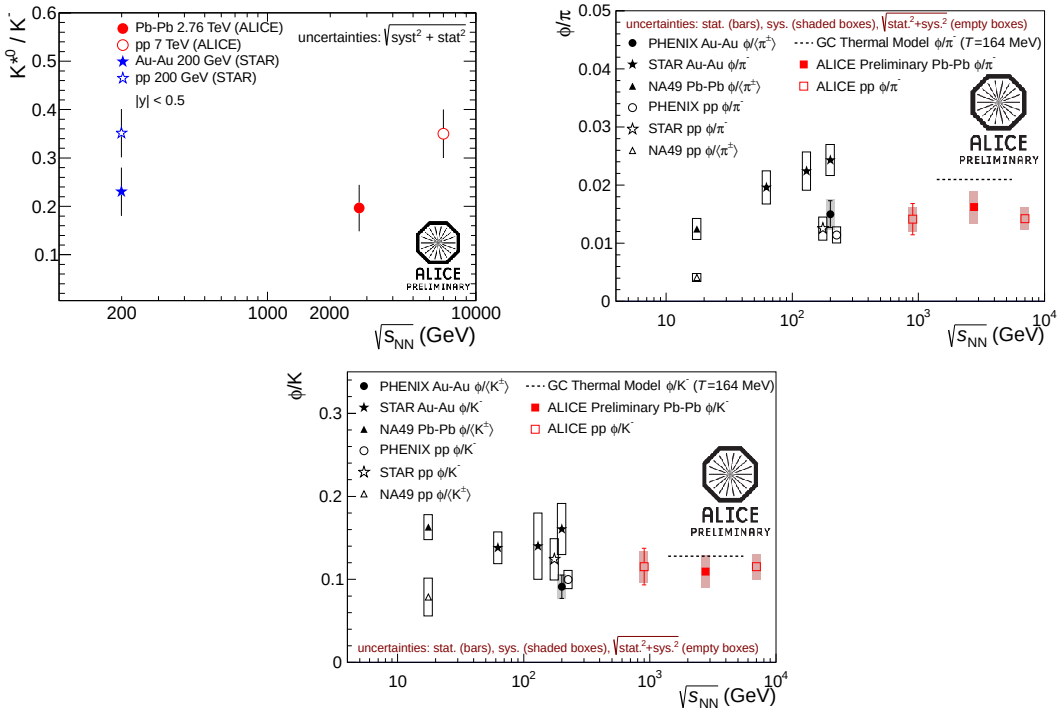

Figure 14: (color online) Energy dependence of the K^*/K^- (left), ϕ/π (right) and ϕ/K (bottom) ratios.

5. Conclusions

The hadronic resonances $K^*(892)^0$, $\phi(1020)$ and $\Sigma(1385)$ have been measured in pp collisions at $\sqrt{s} = 7$ TeV by the ALICE experiment at the LHC. The masses and widths of the resonances are close to the PDG values. Transverse momentum spectra of the $\phi(1020)$ and $\Sigma(1385)$ have been compared to a number of PYTHIA tunes and the PHOJET event generator. None of them gives a fully satisfactory description of the data. For the $\phi(1020)$ meson the latest PYTHIA version (Perugia 2011) comes closest, while still underpredicting p_T spectrum below 3 GeV/c by up to a factor of two. The $\Sigma(1385)$ spectrum is well described by the PYTHIA ATLAS-CSC tune for $p_T > 2$ GeV/c, while other models underpredict the data. The $\langle p_T \rangle$ of the $\phi(1020)$ and $\Sigma(1385)$ is in agreement with the trend drawn by other particles at 7 TeV from ALICE. The K^*/K and ϕ/K^* ratios (and consequently the ϕ/K ratio) are found to be independent of energy up to 7 TeV. Also the ϕ/π ratio, which increases in both pp and A-A collisions up to at least RHIC energies, saturates and becomes independent of energy above 200 GeV. The $(\Omega^- + \overline{\Omega}^+)/\phi$ ratio is not reproduced by PYTHIA Perugia 2011, but is in good agreement with the HIJING/B$\overline{\text{B}}$ v2.0 model with SCF, which enhances multi-strange baryon production by increasing the string tension parameter. The Σ^*/π^- and Σ^*/K^- ratios are independent of energy within errors and agree with the thermal model predictions at $\sqrt{s} = 7$ TeV. The Σ^*/Ξ^- ratio decreases with energy and its value at $\sqrt{s} = 7$ TeV is overpredicted by the thermal model.

The mesonic resonances $K^*(892)^0$ and $\phi(1020)$ have been also measured in Pb-Pb collisions at $\sqrt{s_{NN}}$ = 2.76 TeV. The observed deviations of the masses and widths of the resonances from their vacuum values appear to be due to detector effects. The $\langle p_T \rangle$ of the resonances are higher than that observed at RHIC energies. A weak centrality dependence is observed in the K^*/K^- ratio, while the ϕ/π and ϕ/K ratios are independent of the collision centrality. The decreasing trend in the K^*/K^- ratio suggests a possible increase in rescattering in the most central collisions. The particle ratios ϕ/K, ϕ/π and K^*/K^- are found to be independent of beam energy. The K^*/K^- ratio in Pb-Pb collisions is smaller than that measured in pp collisions. This observation may indicate the effect of hadronic rescatterings at LHC energies. The statistical thermal model prediction for ϕ/K is consistent with the measured value, while the prediction for ϕ/π is larger than the measured value.

References

[1] G. E. Brown and M. Rho, Phys. Rev. Lett. **66**, (1991) 2720. R. Rapp, Nucl. Phys. A **725**, (2003) 254. E. V. Shuryak and G. Brown, Nucl. Phys. A **717**, (2003) 322.

[2] G. Torrieri and J. Rafelski, Phys. Lett. B **509**, (2001) 239.

[3] K. Aamodt *et al.*, (ALICE Collaboration), JINST **3**, (2008) S08002.

[4] C. Tsallis, J. Stat. Phys. **52**, (1988) 479.

[5] E. Schnedermann, J. Sollfrank and U. Heinz, Phys. Rev. C **48** (1993) 2462

[6] K. Aamodt *et al.*, (ALICE Collaboration), arXiv:1208.5717 [hep-ex].

[7] J. Beringer *et al.*, (Particle Data Group), Phys. Rev. D **86**, (2012) 010001.

[8] T. Sjöstrand, S. Mrenna and P. Skands, J. High Energy Phys. **05** (2006) 026.

[9] R. Engel *et al.*, Z. Phys. C **66** (1995) 203; R. Engel and J. Ranft, Phys. Rev. D **54** (1996) 4244.

[10] K. Aamodt *et al.*, (ALICE Collaboration), Eur. Phys. J. C **71** (2011) 1655.

[11] J. Adams *et al.*, (STAR Collaboration), Phys. Rev. C **71** (2005) 064902.

[12] B.I. Abelev *et al.*, (STAR Collaboration), Phys. Rev. C **79** (2009) 064903.

[13] B. Abelev *et al.*, (ALICE Collaboration), Phys. Lett. B **712** (2012) 309.

[14] M. Bourquin and J.M. Gaillard, Nucl. Phys. B **114**, (1976) 334.

[15] H. Albrecht *et al.*, Z. Phys. C**61** (1994) 1.

[16] Y. Pei, Z. Phys. C **72** (1996) 39.

[17] H. Hofmann *et al.*, Ann. Rev. Nucl. Part. Sci. **38** (1988) 279.

[18] K. Abe *et al.*, Phys. Rev. D **59** (1999) 052001.

[19] S. Behrends *et al.*, Phys. Rev. D **31** (1985) 2161.

[20] M. Aguilar-Benitez *et al.*, (LEBC-EHS Collaboration) Z. Phys. C **50** (1991) 405.

[21] D. Drijard *et al.*, Z. Phys. C **9** (1981) 293.

[22] T. Akesson *et al.*, Nucl. Phys. B **203** (1982) 27.

[23] M.M. Aggarwal *et al.*, (STAR Collaboration), Phys. Rev. C **84** (2011) 034909.

[24] B. Abelev *et al.*, (ALICE Collaboration), Measurement of pion, kaon and proton production in pp collisions at 7 TeV, in preparation.

[25] C. Adler *et al.*, (STAR Collaboration), Phys. Rev. C **65** (2002) 041901.

[26] C. Adler *et al.*, (STAR Collaboration), Phys. Rev. C **66** (2002) 061901.

[27] S.S. Adler *et al.*, (PHENIX Collaboration), Phys. Rev. C **72** (2005) 014903.

[28] B.B. Back *et al.*, (E917 Collaboration), Phys. Rev. C **69** (2004) 054901.

[29] S.V. Afanasiev *et al.*, (NA49 Collaboration), Phys. Lett. B **491** (2000) 59.

[30] C. Alt *et al.*, (NA49 Collaboration), Phys. Rev. C **78** (2008) 044907.

[31] K. Adcox *et al.*, (PHENIX Collaboration), Phys. Rev. Lett. **88** (2002) 242301.

[32] A. Adare *et al.*, (PHENIX Collaboration), Phys. Rev. D **83** (2011) 052004.

[33] V. Blobel *et al.*, Phys. Lett. **B59** (1975) 88.

[34] C. Daum *et al.*, Nucl. Phys. B **186** (1981) 205.

[35] J. Adams *et al.*, (STAR Collaboration), Phys. Rev. Lett. **92** (2004) 112301.

[36] A.M. Rossi *et al.*, Nucl. Phys. B **84** (1975) 269.

[37] A. Adare *et al.*, (PHENIX Collaboration), Phys. Rev. C **83**, (2011) 064903.

[38] K. Aamodt *et al.*, (ALICE Collaboration), Eur. Phys. J. C **71** (2011) 1594.

[39] V. Topor Pop *et al.*, Phys. Rev. C **83** (2011) 024902.

[40] N. Armesto *et al.*, J. Phys. G: Nucl. Part. Phys. **35** (2008) 054001.

[41] D. Acosta *et al.*, (CDF Collaboration), Phys. Rev. D **72** (2005) 052001.

[42] V. Topor Pop, private communication.

[43] P.Z. Skands, Phys. Rev. D **82** (2010) 074018.

[44] J. Adams *et al.*, (STAR Collaboration), Phys. Rev. Lett. **97** (2006) 132301.

[45] B.I. Abelev *et al.*, (STAR Collaboration), Phys. Rev. C **75** (2007) 064901.

[46] F. Becattini *et al.*, J. Phys. G **38** 025002 (2011) and private communication

[47] J. Adams *et al.*, (STAR Collaboration), Phys. Lett. B **612** (2005) 181.

[48] H. Sorge Phys. Rev. C **52**,(1995) 3291; M. Bleicher *et al.*, J. Phys G **25**,(1999) 1859; Y. Lu et al J. Phys G **32**,(2006) 1121; B. Mohanty and N. Xu J. Phys G **36**, (2009) 064022.

[49] B. I. Abelev *et al.* (STAR collaboration), Phys. Rev. C **79**,(2011) 64093; A. Adare *et al.* (PHENIX collaboration), Phys. Rev. C **83**,(2011) 64093.

[50] A. Andronic, P. Braun-Munzinger and J. Stachel, J. Phys. G **38**, (2011) 124081.